MRS Communications (2018), 8, 178–182

doi:10.1557/mrc.2018.17

MRS Communications Research Letter

Mechanical finishing and ion beams application to cold working tool steels: consequences for scratch resistance

Witold Brostow, Laboratory of Advanced Polymers & Optimized Materials (LAPOM), Department of Materials Science and Engineering, University of North Texas, 3940 North Elm Street, Denton, TX 76207, USA
Sven Lohse and **Allison T. Osmanson,** Laboratory of Advanced Polymers & Optimized Materials (LAPOM), Department of Materials Science and Engineering, University of North Texas, 3940 North Elm Street, Denton, TX 76207, USA; Ion Beam Modification and Analysis Laboratory (IBMAL), Department of Physics, University of North Texas, 210 Avenue A, Denton, TX 76203, USA
Daniel Tobola, Institute of Advanced Manufacturing Technology (IAMT), Wrocławska 37a, 30-011 Cracow, Poland
Duncan L. Weathers, Ion Beam Modification and Analysis Laboratory (IBMAL), Department of Physics, University of North Texas, 210 Avenue A, Denton, TX 76203, USA

Address all correspondence to Witold Brostow at **wkbrostow@gmail.com**

(Received 15 December 2017; accepted 30 January 2018)

Abstract
We have performed mechanical finishing operations on Sverker 21 (traditional) and Vanadis 6 (advanced powder) steel surfaces: grinding, turning, and turning followed by slide burnishing. Then each specimen was subjected in turn to focused ion beams of helium or krypton up to fluences of 10^{15} ions/cm^2 and finally to scratch resistance testing. Acoustic signals show that krypton implantation reduces microcracks. Helium ions act even more strongly as homogenizers—almost completely eliminating the imperfections. Optical microscopy during scratch testing shows the force level when debris formation begins. Helium ions fitting between the iron atoms increase the resistance against scratching; larger krypton ions produce the opposite effect.

Introduction and scope
There is no need to discuss the width of the range of applications of steels. Tool steels have better properties than ordinary steels, including higher hardness and higher resistance to deformation. There is also a belief that tool steels have higher resistance to abrasion—a belief that we have decided to verify.

There are a variety of methods of improving surface and other properties of steels, including quenching,[1] severe plastic deformation,[2] submerged metal arc welding,[3,4] laser melting,[5–7] shot peening,[8–10] nitriding,[11] electrical discharge machining,[12] or consecutive mechanical treatments followed by nitriding.[13] Thus, in earlier work we have studied turned and burnished (T–B), turned and nitrided (T–N) and turned, burnished and nitrided (T–B–N) steels of two kinds.[13] In [13] we have used pin-on-disk tribometry for the determination of abrasion. We have decided now to investigate the “beginning” of abrasion by scratch resistance testing,[14,15] including the beginning of debris formation. We expected that the acoustic signal accompanying the indenter movement will be useful.

This project started when we acquired access to the capability of ion implantation in steels, namely of helium and krypton. To our knowledge, so-called “rare gases” were never applied to tool steels before. An important advantage of He and Kr are spherical force fields—hence factors other than the atomic mass do not interfere.

Tool steels are classified as “traditional” and “advanced”. We have studied Sverker 21 steel as a representative of the former and Vanadis 6 steel made by powder metallurgy as representing the latter. Both are chromium–molybdenum–vanadium alloyed steels. Vanadis contains hard vanadium and molybdenum carbides—rather than softer chromium carbides. Recall that chromium content allows strengthening of severe plastic deformation.[1] We have 11.8 wt% Cr in the Sverker steel but 6.8% in the Vanadis steel. We have 0.8% V in Sverker but 5.4% in Vanadis.

Experimental
Materials
Sverker 21 and Vanadis 6 were provided by Uddeholms AB, Hagfors, Sweden. They were subjected to heat treatments as follows: Sverker: 270 s at 1035–1040 °C, then 2 h at 530 °C, finally 2 h at 520 °C; Vanadis: 270 s at 1070 °C, 2 h at 550 °C, finally 2 h at 520 °C. Rockwell hardness C (150 kgf, 120° diamond spheroconical indenter) HRC = 60 ± 1 was thus achieved for both.

Mechanical treatments
We have applied three types of operations: grinding (G), turning (T) and turning followed by slide burnishing (T–B). Grinding alone is a known procedure for steels.[16] Grinding

was performed as follows: peripheral wheel speed $v_s = 16$ m/s; table feed speed $v_f = 210$ mm/min and working engagement $a_e = 0.01$ mm. Polycrystalline cubic boron nitride (NP-DCGW11T302GA2 BC020) was used as cutting inserts for turning at the feed of 0.06 mm/rev. with the cutting speed of 100 m/min. for Sverker and 150 m/min. for Vanadis. Different speeds were applied so as to achieve comparable roughness. A diamond was used for slide burnishing with the speed of 40 m/min., feed 0.02 mm/rev. and the force of 180 N for Sverker and 160 N for Vanadis.

Ion implantation

The IBMAL facility has been described earlier[17] and used in a variety of applications.[18] Each of our specimens was subjected in turn to focused 2.5 and 1.5 MeV ion beams of helium and krypton, respectively. The specimens were irradiated a few times with fluences of 10^{15} ions/cm^2.

Scratch testing

The instantaneous depth at the time the indenter "attacks" a given location is called the penetration depth R_p, the depth after 2 min of viscoelastic recovery (healing) is the recovery depth R_h. A linearly increasing force from 0.3 to 22.8 N was applied. A diamond indenter with the diameter of 0.10 µm was used. The depth resolution is ±0.5 nm according to the manufacturer (Anton Paar). The sliding speed was 5 mm/min, the distance covered 5.0 mm. During each test an acoustic signal is created along the indenter trajectory. We provide in the section "Symbols used for specimens" the values of the surface roughness before scratch testing. We recall that surface roughness decreases in tribological testing along with the sliding distance.[19]

Microscopy

After scratch tests were performed, the samples were examined under a microscope which was part of the micro-scratch machine assembly. Panoramic photos were taken of each sample under each condition after scratch testing at 5× magnification.

Symbols used for specimens

Symbols used for specimens are listed in Table I.

Table I. Symbols used for specimens and surface roughness values.

Type of steel	Sample #	Process	Surface roughness Ra/µm
Sverker 21	S21 I	Grinding	0.029
	S21 II	Turning	0.74
	S21 III	Turning + slide burnishing	0.75
			0.16
Vanadis 6	V6 I	Grinding	0.015
	V6 II	Turning	0.72
	V6 III	Turning + slide burnishing	0.70
			0.057

Scratch testing results

Scratch testing provides the instantaneous or penetration depth R_p at the time the indenter "hits" a given location on its path. Materials are known to resist deformation of any kind,[15] hence there is a period of recovery during which the bottom of the groove created by the passage of the indenter goes up. Our repetitive experiments on a variety of materials have shown that the recovery process is completed inside of 2 min; namely, the changes of the depth after 2 min are smaller than 1%. Then we move the indenter applying a very small force to determine the residual depth after recovery—also known as the healing depth R_h. Such determinations are particularly important for shape memory alloys (SMAs).[20]

Values of R_p and R_h are averages for a given material. One usually does three indenter runs and thus obtains the averages. To study more in detail a given groove, one can use the acoustic signal which is measured during the passage of the indenter so that a value exists for each location along the groove. Already in 1980 Wadley et al. noted that "metallurgical variables greatly affect the acoustic emission response of metals".[21] We shall take advantage of this capability.

Below, Fig. 1 displays the penetration depths and residual depths at the maximal loads for one Sverker and one Vanadis steel. According to the MicroScratch Tester manufacturer Anton Paar, the depth resolution is 0.05 nm, hence it cannot be displayed in Fig. 1.

Clearly, the samples treated with helium show the lowest penetration depth whereas krypton increases that depth. Apparently, helium ions increase the resistance against scratching while larger krypton ions produce the opposite effect.

As for the residual depth, untreated Sverker steel has shown the largest value, the Vanadis steel only a small one. Here the advantage of the harder latter steel made by powder metallurgy is seen, while the softer Sverker steel does not resist the indenter "attack" well.

The differences of behavior between helium and krypton-treated samples can be explained by the differences between atomic sizes of helium (31 pm) and krypton (88 pm) ions and the respective sizes of carbon (70 pm) and iron (126 pm) atoms. Helium-treated samples have a tightly packed microstructure, contributing to lower penetration depths and positive viscoelastic recovery. Krypton-treated samples have deeper penetration depth due to internal cohesion weakening in the steels by ions larger than the carbon atoms.

We see a significant viscoelastic recovery in the softer Sverker steel, somewhat less in the Vanadis steel. Polymers are largely known for such recovery, see Chapter 19 in.[15] Such recovery has been seen also in copper pastes.[22] After

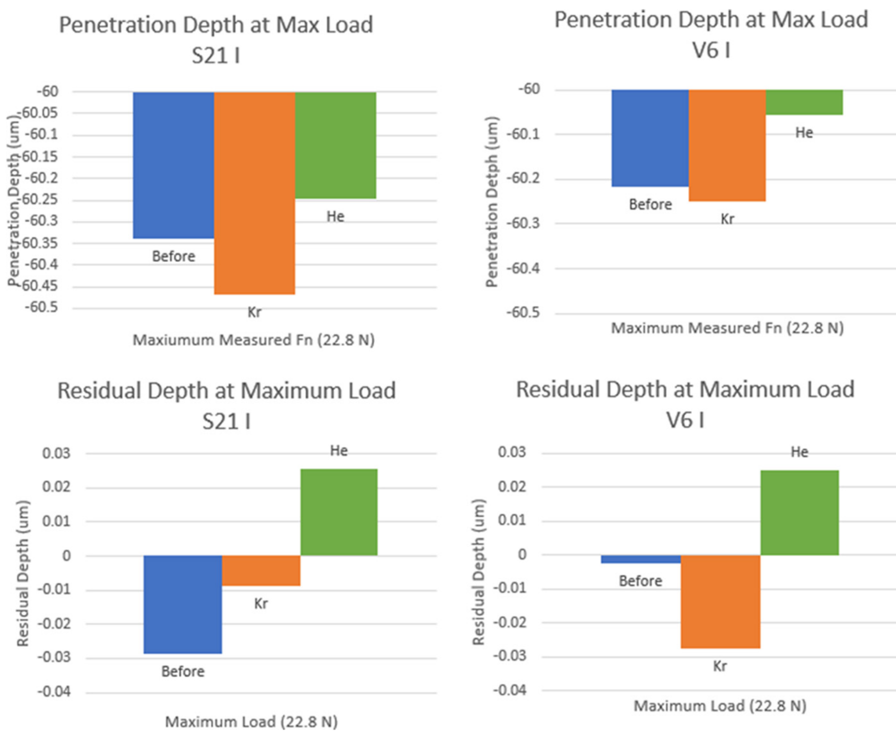

Figure 1. Selected scratch testing results.

the perturbations caused by the indenter, both the steels implanted with krypton ions result in final surfaces above the original ones.

Acoustic emission results

An example pertaining to the sample S21 III is shown in Fig. 2.

Acoustic emission is known to reflect imperfections in the surface such as microcracks—as discussed by Zhou et al.[23] We see that krypton implantation reduces the imperfections. We further see that helium ions act even more strongly as homogenizers—almost completely eliminating the imperfections. These might be examples of material self-organization discussed by Desai and Kapral.[24] A thermodynamic stability criterion tells us that materials attempt to reach equilibrium by lowering their Gibbs function *G*.[15] Crack formation requires increasing *G* since new surfaces are created. Here we have an inverse and natural process involving lowering *G*.

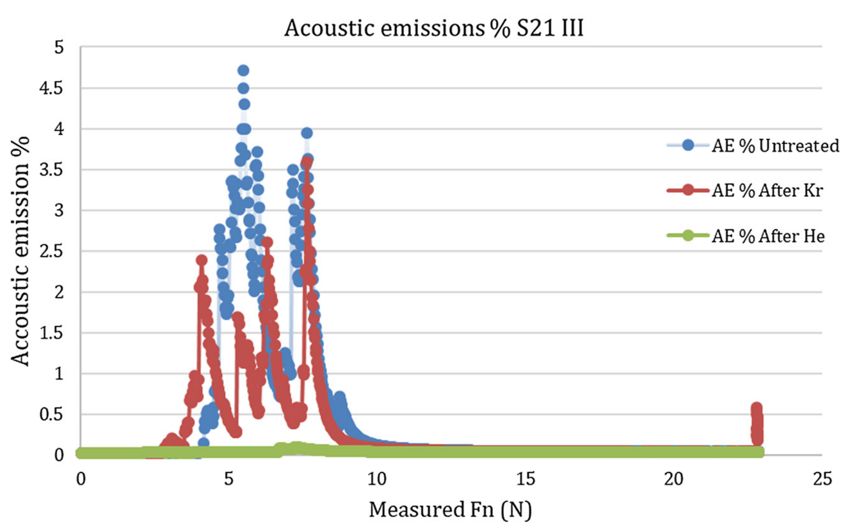

Figure 2. Representation of acoustic emissions.

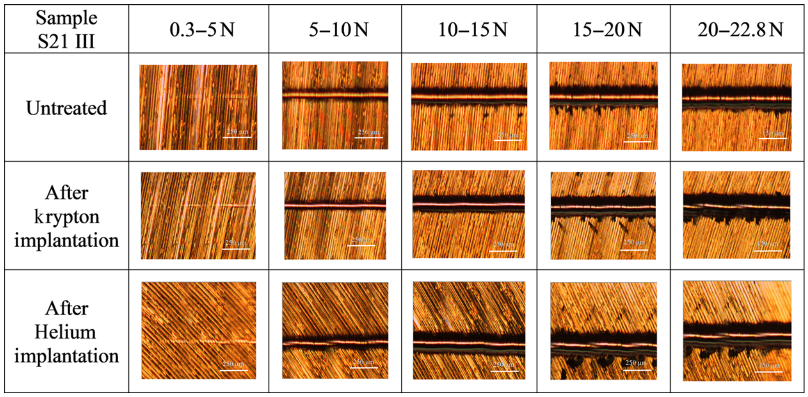

Figure 3. Microscopy images observed for several force level ranges.

At higher force values—above 12 N or so—we see a flat acoustic signal. Apparently, the high force applied eliminates the microcracks by "flattening" them.

The effect of helium or krypton seems different from that of fillers, such as carbon or manganese used to mitigate the effects of welding in steels,[25] or for that matter carbon nanotubes in elastomers.[26,27] The main role of fillers is providing mechanical reinforcement rather than surface homogenization.

Microscopy observations

Advantages of microscopy observations of material surfaces have been extensively discussed by Michler and Balta-Calleja.[28] In Fig. 3, we see images for Sverker 21 III.

We recall first that in Fig. 2 the acoustic events take place particularly between 5 and 15 N of force. Now in Fig. 3, we see a slight scratch on the surface at 5 N, increasing in depth at 10 N, and debris forming at 15 N and beyond for each sample.

Concluding remarks

As already noted, given the importance of steels—and tool steels in particular—there is a variety of methods of improving steel surface properties.[11–13,29–32] While implantation of helium and krypton ions for this purpose has not been used before, the fact that these two kinds of ions produce opposite effects was not expected.

Acknowledgments

The specimens were created and subjected to mechanical treatments under the LIDER/13/0075/L-7/15/NCBR/2016 project funded by the National Center for Research and Development of Poland, Warsaw. Helpful contributions by Jack E. Manuel and Todd Byers at IBMAL-UNT are gratefully acknowledged.

References

1. R. Bendikiene and J. Zvinys: Investigation of transformation plasticity of tempered high chromium steel during quenching. *Mater. Sci. Medziagotyra* **10**, 317 (2004).
2. S.V. Dobatkin, O.V. Rybalchenko, N.A. Enikeev, A.A. Tokar, and M. M. Abramova: Formation of fully austenitic ultrafine-grained high strength state in metastable Cr–Ni–Ti stainless steel by severe plastic deformation. *Mater. Lett.* **166**, 276–279 (2016).
3. P. Ambroza, R. Bendikiene, and L. Kavaliauskiene: Submerged arc surfacing of structural steel using metals powder added to flux. In *Proc. 5th IASME/WSEAS Int. Conf. on Heat Transfer, Thermal Engineering and Environment*, Athens, Greece, 25–27 August 2007, p. 184.
4. R. Bendikiene, E. Pupelis, and L. Kavaliauskiene: Effects of surface alloying and laser beam treatment on the microstructure and wear behaviour of surfaces modified using submerged metal arc welding. *Mater. Sci. Medziagotyra* **22**, 44 (2016).
5. B. AlMangour, F. Yu, J.-M. Yang, and D. Grzesiak: Selective laser melting of TiC/H13 steel bulk-form nanocomposites with variations in processing parameters. *MRS Commun.* **7**, 84–89 (2017).
6. B. AlMangour, D. Grzesiak, and J.-M. Yang: Selective laser melting of TiB2/H13 steel nanocomposites: influence of hot isostatic pressing post-treatment. *J. Mater. Process. Technol.* **244**, 344–353 (2017).
7. B. AlMangour, D. Grzesiak, and J.-M. Yang: Nanocrystalline TiC-reinforced H13 steel matrix nanocomposites fabricated by selective laser melting. *Mater. Des.* **96**, 150–161 (2016).
8. B. AlMangour and J.-M. Yang: Improving the surface quality and mechanical properties by shot-peening of 17–4 stainless steel fabricated by additive manufacturing. *Mater. Des.* **110**, 914–924 (2016).
9. K. Li, Q. Zheng, Ch Li, B. Shao, D. Guo, D. Chen, J. Sun, J. Dong, P. Cao, and K. Shin: Characterization of surface modification of 347 stainless steel upon shot peening. *Scanning* **2017**, 1–4 (2017).
10. M. Jayalakshmi, B. Ramachandra Bhat, and K. Udaya Bhat: Effect of shot peening coverage on surface nanostructuring of 316L stainless steel and its influence on low temperature plasma-nitriding. *Mater. Perf. Char.* **6**, 561–570 (2017).
11. R.M. Muñoz Riofano, L.C. Castelitti, L.C.F. Canale, and G.E. Totten: Improved wear resistance of P/M tool steel alloy with different vanadium contents after ion nitriding. *Wear* **265**, 57–64 (2008).
12. F.L. Amorim, V.A. Dalcin, P. Soares, and L.A. Mendes: Surface modification of tool steel by electrical discharge machining with molybdenum powder mixed in dielectric fluid. *Int. J. Adv. Manuf. Technol.* **91**, 341–350 (2017).
13. D. Tobola, W. Brostow, K. Czechowski, and P. Rusek: Improvement of wear resistance of some cold working tool steels. *Wear* **382–383**, 29 (2017).
14. W. Brostow, V. Kovacevic, D. Vrsaljko, and J. Whitworth: Tribology of polymers and polymer based composites. *J. Mater. Ed.* **32**, 273–290 (2010).
15. W. Brostow and H.E. Hagg Lobland: *Materials: Introduction and Applications* (John Wiley & Sons, New York, 2017).
16. Z. Ding, B. Li, and S.Y. Liang: Phase transformation and residual stress of Maraging C250 steel during grinding. *Mater. Lett.* **154**, 37–39 (2015).

17. B. Rout, M.S. Dhoubhadel, P.R. Poudel, V.C. Kummari, B. Pandey, N. T. Deoli, W.J. Lakshantha, S.J. Mulware, J. Baxley, J.E. Manuel, J. L. Pacheco, S. Szilasi, D.L. Weathers, T. Reinert, G.A. Glass, J. L. Duggan, and F.D. McDaniel: An overview of the facilities, activities, and developments at the University of North Texas Ion Beam Modification and Analysis Laboratory (IBMAL). In AIP Conf. Proc., 2013, **1544**, p. 11.
18. D. Reyes, M. Camacho, M. Camacho, M. Mayorga, D. Weathers, G. Salamo, Z. Wang, and A. Neogi: Laser ablated carbon nanodots for light emission. *Nanoscale Res. Lett.* **11**, 424 (2016).
19. M. Hanief and M.F. Wani: Effect of surface roughness on wear rate during running-in of En31-steel: model and experimental validation. *Mater. Lett.* **176**, 91–93 (2016).
20. H. Yang, A. Fortier, K. Horne, W. Brostow, and H.E. Hagg Lobland: Shape memory metal alloys in the context of teaching smart materials. *J. Mater. Ed.* **38**, 149–156 (2016).
21. H.N.G. Wadley, C.B. Scruby, and J.H. Speake: Acoustic emission for physical examination of metals. *Int. Metal Rev.* **2**, 41–64 (1980).
22. W. Brostow, T. Datashvili, R. McCarty, and J.B. White: Copper viscoelasticity manifested in scratch recovery. *Mater. Chem. Phys.* **124**, 371 (2016).
23. W. Zhou, Y. He, and X. Lu: Acoustic emission in scratch processes of metals. *Insight* **57**, 635–642 (2015).
24. R.C. Desai and R. Kapral: *Dynamics of Self-organized and Self-assembled Structures* (Cambridge University Press, Cambridge, New York, 2009).
25. R.J. Moat, H.J. Stone, A.A. Shirzadi, J.A. Francis, S. Kundu, A.F. Mark, H. K.D.H. Bhadesia, L. Karlsson, and P.J. Withers: Design of weld fillers for mitigation of residual stresses in ferritic and austenitic steel welds. *Sci. Technol. Welding* **16**, 279–284 (2011).
26. A. Szymczyk: Poly(trimethylene terephthalate-*block*-tetramethylene oxide) elastomer/single-walled carbon nanotubes nanocomposites: synthesis, structure, and properties. *J. Appl. Polym. Sci.* **126**, 796–807 (2012).
27. L.A.S. de Almeida Prado, A. Kopyniecka, S. Chandrasekaran, G. Broza, Z. Roslaniec, and K. Schulte: Crystallinity, thermal stability and mechanical properties of thermoplastic elastomer/carbon nanotube nanocomposites. *Macromol. Mater. Eng.* **298**, 359–370 (2013).
28. G.H. Michler and F.J. Balta-Calleja: *Nano- and Micromechanics of Polymers: Structure Modification and Improvement of Properties* (Hanser Publishers, Munich, Cincinnati, 2012).
29. M. Antonov, I. Hussainova, R. Veinthal, and J. Pirso: Effect of temperature and load on three-body abrasion of cermets and steel. *Tribol. Int.* **46**, 261–268 (2012).
30. C.-M. Karamboiki, A. Mourlas, P. Psyllaki, and J. Sideris: Influence of microstructure on the sliding wear behavior of nitrocarburized tool steels. *Wear* **303**, 560–568 (2013).
31. B. Podgornik, F. Majdic, V. Leskovsek, and J. Vizintin: Improving tribological properties of tool steels through combination of deep-cryogenic treatment and plasma nitriding. *Wear* **288**, 88–93 (2012).
32. M.H. Staia, Y. Pérez-Delgado, C. Sanchez, A. Castro, E. LeBourhis, and E. S. Puchi-Cabrera: Hardness properties and high-temperature wear behavior of nitrided AISID2 tool steel, prior and after PAPVD coating. *Wear* **267**, 1452–1461 (2009).